

Magnetotransport of $\text{La}_{0.5}\text{Ba}_{0.5}\text{MnO}_3$

M. Pȩkała,¹ V. Drozd,^{1,2} J. F. Fagnard,³ Ph. Vanderbemden,³ and M. Ausloos^{4,a)}

¹Department of Chemistry, University of Warsaw, Al. Zwirki i Wigury 101, PL-02-089 Warsaw, Poland

²Department of Chemistry, Kiev National Taras Shevchenko University, 60 Volodymyrska st, Kiev 01033, Ukraine and Center for Study Matter at Extreme Conditions, Florida International University, Miami, Florida 33199, USA

³Montefiore Electricity Institute B28, Université de Liège, B-4000 Liège, Belgium

⁴SUPRATECS, Université de Liège, B5 Sart-Tilman, B-4000 Liège, Belgium

(Received 23 June 2008; accepted 10 October 2008; published online 13 January 2009)

Physical properties of polycrystalline $\text{La}_{0.5}\text{Ba}_{0.5}\text{MnO}_3$ are reported from low temperature (10 K) up to above room temperature. An aim has been to obtain microscopic parameters and to search for the characteristic lengths in terms of which one can discuss the interplay between magnetic, electric, and phonon excitations. The structural and magnetotransport measurements reveal a set of relatively high transition temperatures (near 300 K) between ferromagnetic/metallic and paramagnetic/semiconducting phases. It is found, in particular, that the so-called localization length increases from 0.085 to 0.24 nm when the magnetic field varies from 0 to 8 T. Moreover a “special field value” ~ 0.03 T is observed in the description of the electrical resistance. It cannot be presently distinguished whether it is the signature of a spin reorientation transition in the canted phase or a mere saturation field for aligning magnetic domains. The relatively high magnetoresistance effect ($\approx 55\%$ at 8 T and 10 K) makes the $\text{La}_{0.5}\text{Ba}_{0.5}\text{MnO}_3$ a very interesting material for among others sensor applications. © 2009 American Institute of Physics.

[DOI: [10.1063/1.3032326](https://doi.org/10.1063/1.3032326)]

I. INTRODUCTION

The perovskite manganites of general formula $A_{1-x}M_x\text{MnO}_3$ (A =rare earth, M =divalent atoms) attract considerable attention, especially following the discovery of the so-called colossal magnetoresistance (CMR) observed in the vicinity of an insulator-metal (Mott) transition congruent to a paramagnetic-ferromagnetic (Curie), or paramagnetic-antiferromagnetic (Néel) transition.^{1,2} Some of us have discussed elsewhere that these transitions do NOT occur at the same temperature.³⁻⁵ Strong correlations between (ionic) structure, (electronic) transport, and magnetic properties lead to a sophisticated phase diagram for these manganites,⁶ the presence of many phases, and subsequent inhomogeneities in the microstructure. Electrons, magnetic moments, but also collective excitations, i.e., phonons and magnons all play a role in the observed features.⁷ On the other hand, for applied aspects the occurrence of a significant CMR at low applied magnetic fields is required. It is found in the Ba/La manganite family.^{8,9} We report data and considerations on a specific compound $\text{La}_{0.5}\text{Ba}_{0.5}\text{MnO}_3$ and sort out physical features. We indicate a large change in the localization length at small magnetic fields. We consider that this finding and the rather large value of the magnetoresistance are in favor of considerations to pursue technical work on such materials and use them in, e.g., sensitive low magnetic field sensors.

In Sec. II we recall basic features of the $x=0$ and $x=1$ compound, i.e., LaMnO_3 and BaMnO_3 and recall previous work on $\text{La}_{0.5}\text{Ba}_{0.5}\text{MnO}_3$. In Sec. III are succinctly presented generalities about the present experimental methods. In Sec.

IV magnetic characterization results and electrical ones are presented with a discussion, in relation to other findings in Sec. V, i.e., the data on the magnetoresistance. A conclusion follows in Sec. VI.

II. BASIC MANGANITES

A. LaMnO_3

Properties of the pristine AMnO_3 ($A=\text{La}$) were originally studied in Refs. 10 and 11. Much work has been done later on LaMnO_{3-y} . It is known that LaMnO_3 transforms into a canted spin insulator (CSI), at a Néel–Mott temperature near 160 K, made of ferromagnetic layers being coupled antiferromagnetically along the c -axis. The high temperature phase is paramagnetic and insulatinglike.¹¹ Many studies can be also found on compounds where A is substituted, e.g., by $M=\text{Ca}$ (see, as an example, Ref. 12) or also Sr (see, as an example, Ref. 13). When doping with, e.g., Ca, the low temperature phase becomes metalliclike, due to the presence of percolating electric paths in the system. This is due to the presence of a so-called mixed valence ($\text{Mn}^{3+}/\text{Mn}^{4+}$) in the system, whence leading to an electric instability.

B. BaMnO_3

The BaMnO_{3-y} ($0 \leq y \leq 0.1$) perovskite, much studied by Gonzalez-Calbet and co-workers¹⁴⁻¹⁶ shows several types of crystallites with hexagonal symmetry, for $0.1 \leq y \leq 0.25$, but are rhombohedral for $0 \leq y \leq 0.1$. On the basis that oxygen deficiency is accommodated by the introduction of $\text{BaO}_{2.5}$ cubic layers in the hexagonal close packing of BaMnO_3 , the existence of different crystallographic phases

^{a)}Author to whom correspondence should be addressed. Electronic mail: marcel.ausloos@ulg.ac.be.

can be deduced from the expression $y=0.5N_c/(N_c+N_h)$, where N_c and N_h refer to the number of cubic and hexagonal layers per unit cell, respectively.

Neutron powder diffraction data on BaMnO₃ indicate that the oxide ion vacancies are localized in the hexagonal layers and that the structure consists of chains of face-sharing MnO₆ octahedra, separated by Ba²⁺ cations. At room temperature, $a=0.569\,91(2)$ nm, $c=0.481\,48(2)$ nm, space group $P63/mmc$. At 80 K, $a=0.984\,67(1)$ nm, $c=0.480\,75(1)$ nm, space group $P63cm$.^{17,18}

Long-range antiferromagnetic ordering is apparent as high as 200 K.¹⁸ A structural phase transition introduces a displacement of neighboring chains and reduces the coordination number of Ba²⁺ inducing another magnetic transition at a Néel temperature $T_N=59(2)$ K, below which is found a canting of the ordered magnetic moment $\sim 1.31(5)\mu_B$ per Mn⁴⁺ cation at 1.7 K. Neighboring spins within each chain are antiferromagnetically coupled and lie in a plane perpendicular to [001]. The spin directions associated with the chains at $(1/3, 2/3, z)$ and $(2/3, 1/3, z)$ are rotated by $\pm 120^\circ$ with respect to that of the chain at $(0, 0, z)$.

Recently, Hu *et al.*¹⁹ performed the synthesis of single-crystalline nanorods/nanowires of BaMnO₃. The synthesis clearly yields nanorods with a hexagonal perovskite structure. Resistance measurements show that a (magnetic) phase transition happened at ~ 58 K. Interestingly, the ability to synthesize such nanorod manganites of a desired length should enable detailed investigations of the size-dependent evolution of magnetism, magnetoresistance, nanoscale phase separation, and realization of a magnetic sensor nanodevice.

C. (LaBa)MnO₃

In Ref. 8, Millange *et al.* reported that three types of perovskites can be synthesized in the LaBaMn₂O_{6-x} family by controlling the oxygen pressure, during both synthesis and postannealing. Structural determination from powder neutron diffraction data shows that one form of LaBaMn₂O₆ is cubic ($a=0.3906$ nm), with a disordered distribution of La³⁺ and Ba²⁺ cations, whereas a second form of LaBaMn₂O₆ is tetragonal ($a=0.3916$ nm; $c=0.7805$ nm), with an alternate stacking of lanthanum and barium layers along the c axis. The third form is a tetragonal LaBaMn₂O₅. The LaBaMn₂O₆ forms exhibit a remarkable CMR feature:⁸ T_C is increased from 270 K for the disordered phase to 335 K for the ordered one, probably owing to the La/Ba ordering.

Later on, Cherepanov *et al.*²⁰ found that La_{1-x}Ba_xMnO_{3±y} phases with $0 \leq x \leq 0.10$ possess O-orthorhombic structures (space group $Pnma$) and samples with $0.125 \leq x \leq 0.30$ have rhombohedral structures (space group $R3c$) in Hermann–Mauguin (or international) notation.

The complex situation is basically due to the induced strain resulting from the variation in ionic radius size. The ionic radius of La is equal to 0.116 nm in coordination VIII; that of Ca is 0.112 nm in coordination VIII. Thus substitution by a bigger alkali-earth ion, such as Sr having an ionic radius=0.126 nm in coordination VIII, is of great interest; the more so if there is a substitution by Ba (radius of 0.142 nm in coordination VIII), but this is less common. A change

of $\sim 10\%$ is induced by Ba in the so-called tolerance factor,² while it is only about 3% for La (or Ca). This suggests to study a 50% substitution of Ba on La. It is expected that a stable crystallographic phase exists as up to 40% substitution, beyond which mixed phases of LaMnO₃ and BaMnO₃ are formed¹⁰ although data on a single phase, apparently La_{0.54}Ba_{0.46}MnO₃, has been reported.²¹

A discussion of physical properties of some La_{1-x}Ba_xMnO₃ can be found in Refs. 22–27 on polycrystalline materials for various concentrations or on films.^{28,29} For completeness, see reporting results sometimes on properties not examined here, i.e., like the Hall effect.³⁰

Therefore despite the long lasting scientific interest in magnetoresistive manganites, there is a very scarce characterization of the La_{1-x}Ba_xMnO₃ system. The present paper is aimed at a deeper characterization of the La_{0.5}Ba_{0.5}MnO₃ physical, i.e., magnetic and electrical, properties. We will consider the 0.50–0.50 case which formally has equal densities of Mn³⁺ and Mn⁴⁺ ions.

III. EXPERIMENTAL

A. Synthesis and structural determination

Samples of La_{0.5}Ba_{0.5}MnO_{3-y} were prepared by the carbonate coprecipitation method described previously.³¹ Powder x-ray diffraction (XRD) was carried out using high-resolution angle-dispersive synchrotron source at Cornell High Energy Synchrotron Source (CHESS). The synchrotron source was operated at a wavelength of 0.619 921 Å with the Ge crystal (111) orientation. XRD patterns were collected in transmission geometry spinning the sample in a sample holder to avoid spurious effects due to the powder polycrystallinity. Several two-dimensional diffraction images collected by image plate were integrated using the FIT2D program.³² The Rietveld refinement of the powder XRD data were carried out using GSAS program.^{33,34}

A phase analysis of a La_{0.5}Ba_{0.5}MnO₃ sample has revealed the presence of a secondary Ba₄Mn₃O₁₀ phase (ICSD 051-1784). Its weight fraction estimated by GSAS fitting was 4.4 wt %.

It is well known that ordering of Ba and La atoms leads to a tetragonal structure with doubled c axis.^{35,36} We do not see any additional peak on the XRD pattern which could reveal such an effect. There is also no phase separation like a cubic LaMnO₃ and/or a hexagonal Ba.

The results of a Rietveld refinement of a La_{0.5}Ba_{0.5}MnO₃ sample are shown in Fig. 1. The XRD pattern of La_{0.5}Ba_{0.5}MnO₃ phase was fitted to data on the primitive cubic perovskite (space group $Pm-3m$) structure. The refined lattice parameter $a=0.390\,770(6)$ nm and the unit cell volume $V=0.059\,671(2)$ nm³. These values are perfectly in agreement with those reported by Nakajima *et al.*^{37,38} However the structural data reveal that in the studied manganites the MnO₆ octahedra are not tilted and the apical O–Mn–O angles are equal to 180°. The oxygen content does not differ more than 0.01 from the stoichiometric one according to iodometric titration.

The scanning electron micrographs show a spongelike structure with unit cross section approximately below

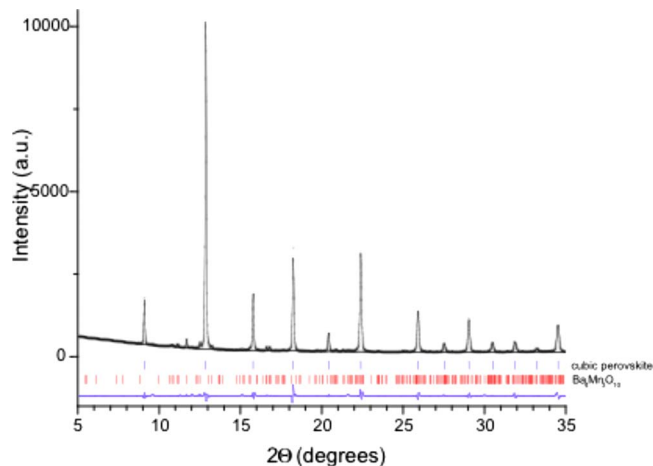


FIG. 1. (Color online) Observed intensities and calculated intensities from Rietveld refinement (upper line) of $\text{La}_{0.5}\text{Ba}_{0.5}\text{MnO}_3$ sample. Positions of Bragg reflections are shown with bars for the cubic perovskite phase and $\text{Ba}_4\text{Mn}_3\text{O}_{10}$. The difference between observed and calculated intensities is shown on the bottom line.

500 nm² (Fig. 2). The average size of the grains is visually of the order of a few micrometers. The structure details are described separately.³¹ The size variance (disorder) of the A cation radius distribution parameter σ^2 for $\text{La}_{0.5}\text{Ba}_{0.5}\text{MnO}_3$ is 0.000 161 nm², as calculated by the formula

$$\sigma^2(R_A) = \sum_i y_i R_i^2 - R_A^2, \quad (1)$$

where y_i , R_i , and R_A stand for the fraction and radius of the i or A cation, respectively.³⁹ The σ^2 value is not much different from that one reported by Raveau *et al.*⁴⁰

B. Physical properties determination

The low field magnetization measurements were performed in a 10 mT magnetic field, whereas the ac magnetic susceptibility was registered at 0.1 mT amplitude, in a physical property measurement system (PPMS). The four probe method was used to measure the electrical resistivity, the applied magnetic field going up to 8 T, by 1 T steps. It was

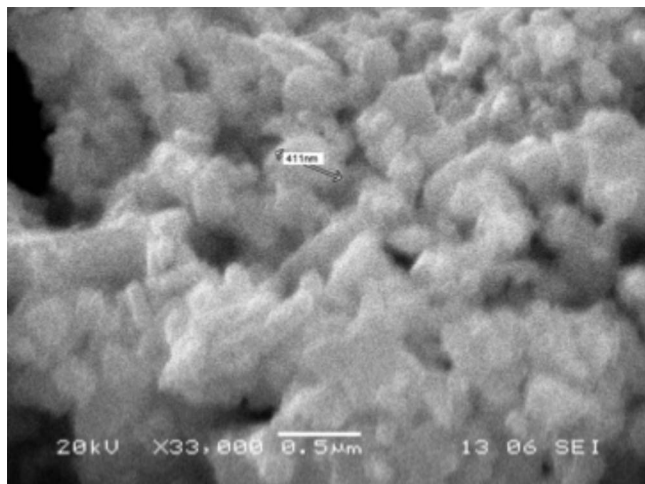


FIG. 2. Scanning electron micrograph of spongelike microstructure of a $\text{La}_{0.5}\text{Ba}_{0.5}\text{MnO}_3$ sample.

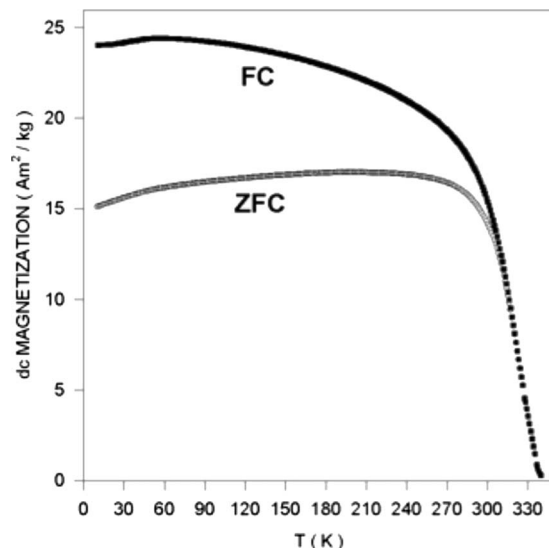


FIG. 3. Temperature variation of the FC and ZFC magnetizations measured at 100 Oe for a $\text{La}_{0.5}\text{Ba}_{0.5}\text{MnO}_3$ sample.

applied under the standard zero-field-cooled (ZFC) technique, i.e., an experimental run ends after heating to (above) room temperature, the field is removed, the sample cooled down to 10 K when a larger field is applied, before starting a new run; the temperature was changed with a mean rate of 1 K/min up to (above) room temperature. The cooling rate is about 8 K/min though we set 20 K/min to the PPMS.

IV. RESULTS

A. Magnetic characterization

The temperature variation of the low field (10 mT) dc magnetization and the ac magnetic susceptibility are shown in Figs. 3 and 4. It is seen that the $\text{La}_{0.5}\text{Ba}_{0.5}\text{MnO}_{3-y}$ remains ferromagnetic well above room temperature. Moreover notice some mild feature at low temperature, i.e., a change in

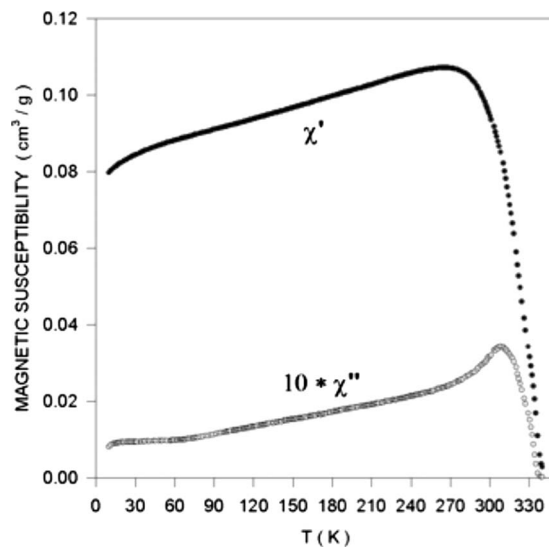


FIG. 4. Temperature variation of the in-phase χ' and out-of-phase χ'' ac magnetic susceptibility of a $\text{La}_{0.5}\text{Ba}_{0.5}\text{MnO}_3$ sample.

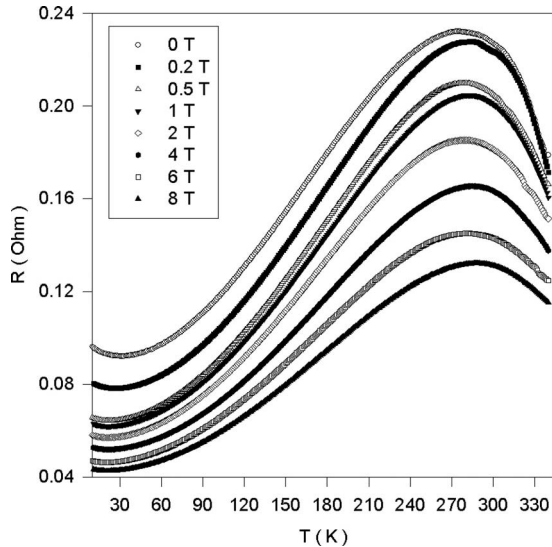


FIG. 5. Temperature variation of the electrical resistance of this $\text{La}_{0.5}\text{Ba}_{0.5}\text{MnO}_3$ sample measured at various magnetic fields.

curvature in $M(T)$; it reminds us that resistance measurements show that a (magnetic) phase transition happens at 58 K in BaMnO_3 .^{17,19}

The pronounced split between the field-cooled (FC) and ZFC curves registered in a 10 mT field is observed to occur below what is called the irreversibility temperature $T_{\text{IR}} \approx 308$ K. We do not enter the debate on whether the transition is first or second order in this work. One may notice that the out-of-phase component of the magnetic susceptibility attains its maximum near the transition temperature.

B. Electrical resistivity in high magnetic fields

The temperature variation of the electrical resistance of $\text{La}_{0.5}\text{Ba}_{0.5}\text{MnO}_{3-y}$ is plotted in Fig. 5 for magnetic field varying up to 8 T. The electrical resistivity is of the order of $2 \times 10^{-4} \Omega \text{ m}$ at room temperature in zero field.

The electrical resistivity peak separating the metallic and semiconducting phases shifts from $T_p=274$ to 288 K when the magnetic field is changed from 0 to 8 T.

V. DISCUSSION

A. Magnetic properties

The Curie temperature T_C determined by the maximum slope in the temperature variation of χ' is found to be equal to 323 K. Such an elevated T_C value confirms the high oxygen content²⁴ or/and is due to an excellent ordering of the Ba and La ions and correlates with the high value of the so-called tolerance factor $f=1.026$.³⁷ Moreover, it should be noticed that the ferromagnetic ordering in $\text{La}_{0.5}\text{Ba}_{0.5}\text{MnO}_{3-y}$ is observed, despite some predictions⁴¹ that a spin glass phase may dominate, when the variance σ^2 of A-cation distribution exceeds 0.0001 nm^2 .^{37,40,41} The ferro- to paramagnetic transition occurs in a narrow temperature interval (about 20 K) revealing a high homogeneity of the samples.

It is worth to recall that A-site ordered and disordered forms of $\text{La}_{0.5}\text{Ba}_{0.5}\text{MnO}_{3-y}$ both have the same Curie temperature.⁴² Therefore it is not possible to distinguish,

which form dominates in the samples studied here. On the other hand there are also papers which report T_C equal to 350 and 300 K for ordered and disordered phases, respectively, e.g., in the polycrystalline $\text{La}_{0.54}\text{Ba}_{0.46}\text{MnO}_3$.²¹

Below this temperature regime, one observes (Fig. 3) in the real part of the magnetic susceptibility a departure from linearity at 308 K, corresponding to a peak in the imaginary part of the susceptibility. Later on, below 274 K the real and imaginary parts of the susceptibility rebecome linear down to 70 K or so at which both components have a change in curvature. This temperature can be as done by others attributed to an antiferromagnetic transition, well marked on the FC and ZFC data for the magnetization (Fig. 4), near 55 K. On this data one also remarks the presence of a change in slope at 308 K, a maximum slope at 325 K, and the magnetization disappearance at 335 K. The tiny upper part of the curve indicates the possible existence of magnetic domains, likely in the larger grains.

The low temperature reduction in the magnetic susceptibility and the field-cooled magnetization reveal a competing magnetic ordering of possibly spin glass type, but it might be also representative of grains with various magnetic orientations. The latter being likely more probable here due to the small grain size. See also Fig. 1 in Ref. 22 where a marked change in curvature is observed below the main critical region.

B. Electrical properties

The electrical resistivity shows a complex variation, decreasing from low temperature, going through a minimum and a maximum before decreasing again at high temperature. The sharpness of the evolution near the peak is usually interpreted as due to the lattice distortion, as should be expected here. The overall shape indicates the presence of a multigrain structure with probably unstable magnetic domains.⁴³ Let us observe that the ratio of electrical resistivity values at the peak and at low temperature is about 3, i.e., a typical value for polycrystalline manganites.⁴⁴ The resistivity minimum, at 30 K in absence of magnetic field, shifts toward zero temperature and finally vanishes in high magnetic fields. Notice that the low temperature residual resistivity decreases more than twice when the magnetic field varies from 0 to 8 T.

The low temperature resistivity minimum origin is controversial. It is sometimes considered to be due to the grains of smallest size^{2,44-46} inducing electron localization. Nevertheless recall that resistance measurements show a magnetic phase transition to happen at 58 K in BaMnO_3 .

Assuming the validity of Matthiessen rule,^{47,48} the full temperature dependence of the electrical resistivity might be written as a linear superposition of various temperature dependent terms representing various electron, phonon, magnon, scattering mechanisms, i.e., residual, impurities, grain boundaries, phonon ($\sim T$) above the Debye temperature, electron ($\sim T^2$), ferromagnetic magnon ($\sim T^{9/2}$), phonon ($\sim T^5$) below the Debye temperature, etc. Recall that the De-

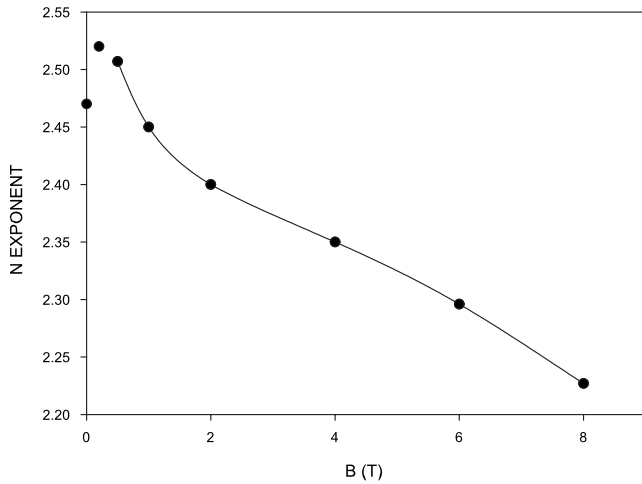


FIG. 6. Magnetic field dependence of the N exponent of the temperature variation of the electrical resistivity below T_C for a $\text{La}_{0.5}\text{Ba}_{0.5}\text{MnO}_3$ sample; a spline function is used as a guide for the eye on the last six data points.

bye temperature is of the order of 300–700 K in manganites, thus much above the temperature regime hereby investigated.

It is hardly conceivable to extract all the contributions from the resistivity data, and to make some sense of the coefficient values, without drastic approximations. Thus a “global,” one exponent formula is used.¹¹ In the medium temperature metalliclike phase the electrical resistivity may be fitted to

$$R(T) = R_0 + A_N T^N \quad (2)$$

from which N is extracted and should be interpreted. Values of the N exponent as plotted in Fig. 6 exhibit a relatively small but undubious maximum ($N=2.52$) near/below a 1 T magnetic field and monotonically diminish with increasing magnetic field values; a spline function fit serves as a guide for the eye. Our values differ much from those of Ref. 25 where it was found that $N \approx 0.75-1.00$ for samples with very low Ba content.

The 0.3 T field at the maximum can be thought as some “critical field” at which the magnetic domains tend to align along the field direction. Inside a magnetic domain the $\text{Mn}^{3+}/\text{Mn}^{4+}$ pairs allow for an easy transfer of electrons⁴³ which becomes more temperature dependent due to fluctuations when the system approaches the magnetic transitions. However the $H=0.3$ might also have a more microscopic origin. Rather than the magnetic saturation field²⁴ which should be temperature dependent the field could be the signature of a critical field at which a spin reorientation transition occurs in the canted antiferromagnetic phase. A third possibility would be a strong effect on the grain boundary scattering mechanism, through some destruction of a lack of coherence of the electronic wave function through the inter-grain barrier. See the argument continuing in Sec. V C on the magnetoresistance.

Other temperature components can be imagined,^{47,48} i.e., a T or T^5 , at high or low temperature, as in Gruneisen law—the regime of validity depending on the Debye temperature, ~ 400 K.⁴⁸ However the deconvolution parameters of a

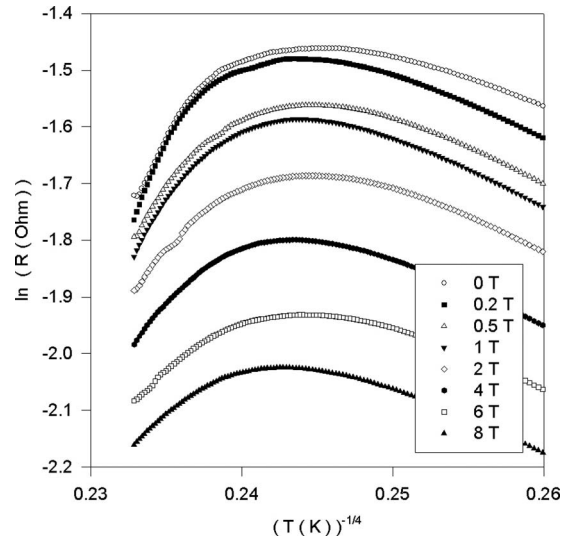


FIG. 7. Mott plot of the temperature variation of the electrical resistance of this $\text{La}_{0.5}\text{Ba}_{0.5}\text{MnO}_3$ sample measured in various magnetic fields.

(supposedly linear) combination, according to Mathiessen rule, could hardly be interpreted due to the complexity of the grain inner structure and the polygranular nature of the samples. It could also finally be discussed whether a Gruneisen form can be used for the background, in view of the grain boundaries requesting some complex averaging. Therefore we accept Eq. (2) as a rough approximation, nevertheless observing that the derived N values spread between 2 and 2.5, most likely revealing a superposition of several scattering mechanisms. However the diminishing variation of N values in Fig. 6, clearly shows that the electron-magnon scattering is reduced in strong magnetic fields, which causes a high level of mutual ordering among the Mn magnetic moments. It is also worth to notice that in contrast to single crystals, values of the peak temperature T_p are lower as compared to the Curie temperature T_C (Ref. 49) and as discussed in Refs. 3 and 4.

In the semiconducting phase (Fig. 7) the electrical resistivity behavior was found to be best fitted to the expression corresponding to the variable range hopping^{50,51}

$$R(T) = R_W e^{(T_0/T)^{1/\nu}}, \quad (3)$$

where ν is dimension dependent; $\nu=4$ in three dimensions.

The T_0 and R_W plots as a function of the field reveal some irregularity below 1 T, as for N (Fig. 6). Fit functions valid at high field are indicated in the captions of Figs. 8 and 9 and serve to quantify the parameter values. They are comparable to those reported for similar manganites.^{28,52-54} Notice the specific B power law dependence for the derived T_0 and R_W parameters. For the three dimensional case, T_0 is related to the density of states at the Fermi level $N(E_F)$ and to the localization length L as follows:^{28,55}

$$T_0 = \frac{24}{k_B N(E_F) \pi L^3}. \quad (4)$$

Then, in absence of data from the Hall coefficient, we rely on assuming that in manganites the density of states $N(E_F)$ is about 2.4×10^{28} (eV m^3)⁻¹.⁵⁶ This allows one to estimate

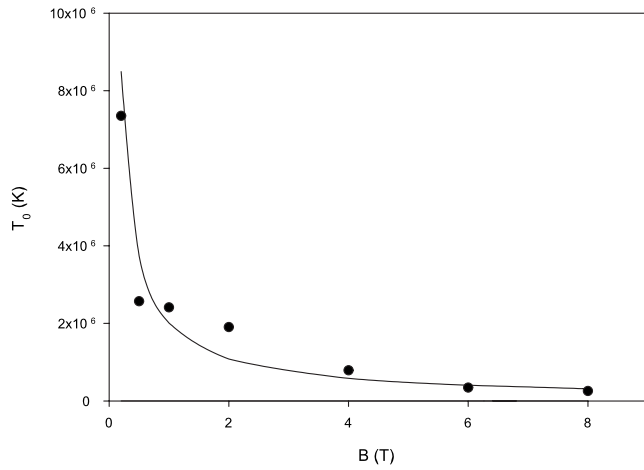


FIG. 8. Magnetic field dependence of the T_0 parameter of the variable range hopping model; the interpolating curve is a guide for the eye only, but corresponds to $T_0 = 2 \times 10^6 B^{-0.85}$.

the localization length L to be about 0.085 nm in absence of field. At higher magnetic fields T_0 is a decreasing function of magnetic field (Fig. 8) and shows that the localization length L rises with the applied magnetic field strength, achieving 0.24 nm at 8 T. Such a localization length is comparable to 0.07 nm reported for $\text{La}_{0.7}\text{Ba}_{0.3}\text{MnO}_3$ thin film manganite³⁰ and to 0.045 nm for $\text{La}_{0.70}\text{Sr}_{0.30}\text{MnO}_3$.⁵⁷ The opposite tendency is observed for the R_W parameter, which is enhanced by the magnetic field (Fig. 9).

Alternatively the experimental resistivity (in fact, resistance) can be also fitted to the nonadiabatic small polaron model of electron conduction⁵⁸

$$R(T) = A_p T^\alpha e^{E_A/(k_B T)}, \quad (5)$$

where E_A is an energy of small polaron activation, where α is often taken equal to 1 assuming an adiabatic regime. However this leads to unphysically low values of the activation energy E_A according to other studies of manganites.^{59,60}

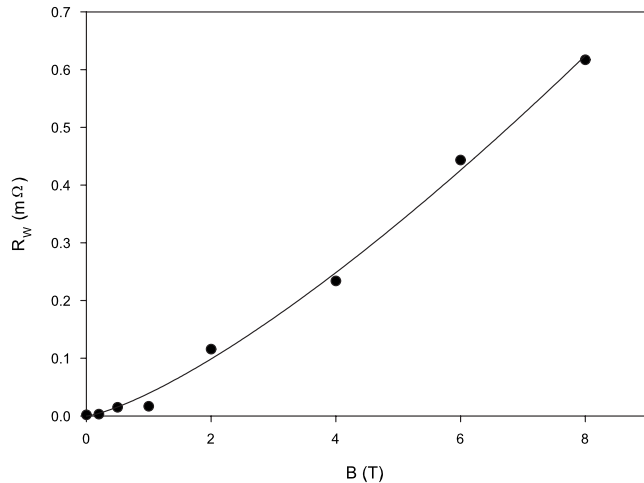


FIG. 9. Magnetic field dependence of the R_W (mΩ) parameter of the variable range hopping model; the interpolating curve is a guide for the eye only, but corresponds to $R_W = 0.04 B^{1.33}$.

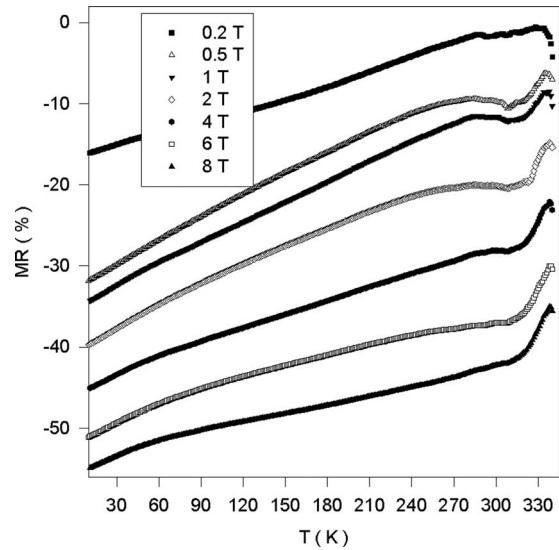


FIG. 10. Temperature variation of the magnetoresistance measured at various magnetic fields.

C. Magnetoresistance

Even though our interest stems in the low field regime, for practical applications, it is of interest to observe the CMR in not too low fields. This allows some information on intra- and intergrain effects indeed.⁶¹

An important information on magnetoresistive materials is supplied by the magnetoresistance defined as

$$\text{MR} = - \left[1 - \frac{R(H)}{R(H=0)} \right], \quad (6)$$

where $R(H)$ and $R(H=0)$ correspond to the electrical resistivity value in finite magnetic fields H and in $H=0$, respectively. Figure 10 shows that the absolute value of MR increases in strong magnetic fields up to 55% at 8 T. At temperatures below T_C this points out to the enhanced ordering of the Mn^{3+} and Mn^{4+} spins likely at magnetic domain boundaries, by the external magnetic field. The temperature variation of MR is most abrupt above room temperature. In this temperature interval an interesting trace of MR minimum around 310 K is observable only at weaker magnetic fields. This effect is related to the ordering of manganese spins in the paramagnetic phase, which is proportional to magnetic field strength. Below 280 K values of MR increase approximately linearly with lowering the temperature down to 10 K.

Notice in this respect the change in behavior of the MR at $H \sim 0.3$ T, congruent to the lack of feature at low temperature below the Néel temperature. It does not seem apparent that the overall shape of the resistance changes much when the field is modified, indicating that the magnetic domains are rapidly aligned, and domain boundary resistance having an equivalent value. The position of the minimum and the decrease in localization of the carriers [$R(T)$ decreases with increasing T] might indicate a microscopic intragrain effect, such as a spin reorientation transition. We substantiate the argument in pointing out that the magnetization and susceptibility have a mild feature at low temperature in a field below 0.3 T (Figs. 3 and 4).

VI. CONCLUSION

Here above magnetic and electrical properties of an unusual magnetoresistive manganite, in a polycrystalline form, have been reported. It is known that the physical properties of such compounds differ whether they are measured on polycrystalline, films or single crystals. Much strain is expected because of the ion radius difference between Mn and the divalent metals on one hand, and that between Ba and La, on the other hand. Moreover the variation in critical temperature(s) is known to be wide, much depending on the Ba/La ordering. However there is more to examine in such materials than the critical temperature(s).

Thus, the phase content has been examined. The presence of a 4.4 wt % $\text{Ba}_4\text{Mn}_3\text{O}_{10}$ impurity phase is observed which implies that the composition of the perovskite phase shifts to a La-rich region, i.e., $\text{La}_{0.5+y}\text{Ba}_{0.5-y}\text{MnO}_3$. This corroborates reports by Chakraborty and co-workers.^{25,26} Thus the incommensurate ratio of La/Ba concentrations should suggest some not too high Curie temperature, and the possible presence of several transition temperatures if the grains are not homogeneous. Ju *et al.*²⁴ studied the effect of oxygen content on the same properties as here for the $y=0.17$ compound. Data comparison shows that the studied samples were highly oxygenated.

However a comprehensive magnetic and transport investigation reveals one relatively high transition temperature between the ferromagnetic/metallic and paramagnetic/semiconducting phases. This implies a rather homogeneous grain composition, as guessed from the structural x-ray analysis, irrespective of the magnetic content and behavior. It seems also that the synthesis technique leads to ordered samples.^{8,42} Yet the magnetic features appear to be complex; several shoulders or change in slope in the magnetization and the susceptibilities indicate several temperature regimes.

The electrical resistance as measured in fields below 8 T has also a complex behavior reminiscent of the coexistence of band and localized carriers and magnetic domains.^{24,43} The temperature dependence roughly goes as $T^{2.5}$, indicating an interplay between different scattering mechanisms. Their relative weight has not been examined because they would lead to a set of parameters hardly reconcilable with theoretical work. However in the magnetoresistance we observe a change in curvature behavior for the data between 0.2 and 0.5 T, thus suggesting a critical field near 0.3 T which can be conjectured to correspond to a reorientation field for the magnetic moments in the magnetic-metallic phase, sometimes called a saturation field as well. The insulating behavior has been examined. We have concluded that the electronic system is characterized by a localization length which increases from 0.085 to 0.24 nm when the magnetic field increases from 0 to 8 T.

Finally, the comprehensive structural and magnetotransport investigations reveal a relatively high transition temperature between the ferromagnetic/metallic and paramagnetic/semiconducting phases. The relatively high magnetoresistance effect makes $\text{La}_{0.5}\text{Ba}_{0.5}\text{MnO}_{3-y}$ an interesting material, e.g., in low field sensor applications.

ACKNOWLEDGMENTS

The authors would like to thank R. Cloots, J. Mucha, and B. Vertruyen for their interest and comments. This work was partially supported by the Ministry of Science and Higher Education (PL Grant No. WAL/286/2006), CGRI (B) and Kasa Mianowskiego (PL). Cryofluids could be bought due to financial support from FNRS-CREDIT AUX CHERCHEURS 1.5.276.07. This work was based upon research conducted at the CHESS which is supported by the National Science Foundation and the National Institutes of Health/National Institute of General Medical Sciences under NSF Award No. DMR-0225180.

- ¹R. M. Kusters, J. Singleton, D. A. Keon, R. M. Greedy, and W. Hayes, *Physica B* **155**, 362 (1989).
- ²J. M. D. Coey, M. Viret, and S. von Molnar, *Adv. Phys.* **48**, 167 (1999).
- ³S. Sergeenkov, H. Bougrine, M. Ausloos, and A. Gilibert, *JETP Lett.* **70**, 141 (1999).
- ⁴S. Sergeenkov, H. Bougrine, M. Ausloos, and A. Gilibert, *Phys. Rev. B* **60**, 12322 (1999).
- ⁵Ph. Vanderbemden, M. Ausloos, G. Dhalenne, R. Cloots, A. Rulmont, and B. Vertruyen, *Phys. Rev. B* **68**, 224418 (2003).
- ⁶P. Schiffer, A. P. Ramirez, W. Bao, and S.-W. Cheong, *Phys. Rev. Lett.* **75**, 3336 (1995).
- ⁷M. Ausloos, L. Hubert, S. Dorbolo, A. Gilibert, and R. Cloots, *Phys. Rev. B* **66**, 174436 (2002).
- ⁸F. Millange, V. Caignaert, B. Domenges, B. Raveau, and E. Suard, *Chem. Mater.* **10**, 1974 (1998).
- ⁹T. Nakajima, H. Kageyama, H. Yoshizawa, K. Ohoyama, and Y. Ueda, *J. Phys. Soc. Jpn.* **72**, 3237 (2003).
- ¹⁰A. Chakraborty, P. Sujatha Devi, and H. S. Maiti, *J. Mater. Res.* **10**, 918 (1995).
- ¹¹L. M. Rodriguez-Martinez and J. P. Attfield, *Phys. Rev. B* **58**, 2426 (1998).
- ¹²B. Raveau, Y. M. Zhao, C. Martin, M. Hervieu, and A. Maignan, *J. Solid State Chem.* **149**, 203 (2000).
- ¹³F. Damay, A. Maignan, C. Martin, and B. Raveau, *J. Appl. Phys.* **81**, 1372 (1997).
- ¹⁴J. M. Gonzalez-Calbet, M. Parras, J. Alonso, and M. Vallet-Regi, *J. Solid State Chem.* **111**, 202 (1994).
- ¹⁵M. Parras, J. M. Gonzalez-Calbet, J. Alonso, and M. Vallet-Regi, *J. Solid State Chem.* **113**, 78 (1994).
- ¹⁶J. M. Gonzalez-Calbet, M. Parras, J. Alonso, and M. Vallet-Regi, *J. Solid State Chem.* **106**, 99 (1993).
- ¹⁷E. J. Cussen and P. D. Battle, *Chem. Mater.* **12**, 831 (2000).
- ¹⁸J. J. Adkin and M. A. Hayward, *J. Solid State Chem.* **179**, 70 (2006).
- ¹⁹C. G. Hu, H. Liu, C. S. Lao, L. Y. Zhang, D. Davidovic, and Z. L. Wang, *J. Phys. Chem. B* **110**, 14050 (2006).
- ²⁰V. A. Cherepanov, E. A. Filonova, V. I. Voronin, and I. F. Berger, *J. Solid State Chem.* **153**, 205 (2000).
- ²¹T. J. Sato, J. W. Lynn, and B. Dabrowski, *Phys. Rev. Lett.* **93**, 267204 (2004).
- ²²W. Li, H. P. Kunkel, X. Z. Zhou, G. Williams, Y. Mukovskii, and D. Shulyatev, *Phys. Rev. B* **70**, 214413 (2004).
- ²³J. J. Hamilton, E. L. Keatley, H. L. Ju, A. K. Raychaudhuri, V. N. Smolyaninova, and R. L. Greene, *Phys. Rev. B* **54**, 14926 (1996).
- ²⁴N. L. Ju, J. Gopalakrishnan, J. L. Peng, and Q. Li, G. C. Xiong, T. Venkatesan, and R.L. Greene, *Phys. Rev. B* **51**, 6143 (1995).
- ²⁵A. Chakraborty, D. Bhattacharya, and H. S. Maiti, *Phys. Rev. B* **56**, 8828 (1997).
- ²⁶D. Bhattacharya, P. Das, A. Paandey, A. K. Raychaudhuri, A. Chakraborty, and V. N. Ojha, *J. Phys. C* **13**, L431 (2001).
- ²⁷J. M. D. Coey, M. Viret, L. Ranno, and K. Ounadjela, *Phys. Rev. Lett.* **75**, 3910 (1995).
- ²⁸M. Ziese and C. Srinithiwarawong, *Phys. Rev. B* **58**, 11519 (1998).
- ²⁹R. von Helmolt, J. Wecker, B. Holzapfel, L. Schultz, and K. Samwer, *Phys. Rev. Lett.* **71**, 2331 (1993).
- ³⁰M. Ziese and C. Srinithiwarawong, *Europhys. Lett.* **45**, 256 (1999).
- ³¹M. Pekała, V. Drozd, J. Kovac, and I. Skorvanek, *Czech. J. Phys.* **54** (Suppl. D), D415 (2004).

- ³²A. P. Hammersley, ESRF Internal Report No. ESRF97HA02T, 1997.
- ³³A.C. Larson and R.B. Von Dreele, Los Alamos National Laboratory Report No. LAUR 86, 2004.
- ³⁴B. H. Toby, *J. Appl. Crystallogr.* **34**, 210 (2001).
- ³⁵T. Nakajima, H. Kageyama, H. Yoshizawa, K. Ohoyama, and Y. Ueda, *J. Phys. Soc. Jpn.* **72**, 3237 (2003).
- ³⁶Y. Ueda and T. Nakajima, *J. Phys.: Condens. Matter* **16**, S573 (2004).
- ³⁷T. Nakajima, H. Yoshizawa, K. Ohoyama, and Y. Ueda, *J. Phys. Soc. Jpn.* **73**, 2283 (2004).
- ³⁸T. Nakajima and Y. Ueda, *J. Alloys Compd.* **383**, 135 (2004).
- ³⁹L. M. Rodriguez-Martinez and J. P. Attfield, *Phys. Rev. B* **54**, R15622 (1996).
- ⁴⁰B. Raveau, A. Maignan, C. Martin, and M. Hervieu, in *Colossal Magnetoresistance, Charge Ordering and Related Properties of Manganese Oxides*, edited by C. N. R. Rao and B. Raveau (World Scientific, Singapore, 1998), p. 43.
- ⁴¹A. Maignan, C. Martin, F. Damay, B. Raveau, and J. Hejtmanek, *Phys. Rev. B* **58**, 2758 (1998).
- ⁴²D. Akahoshi, M. Uchida, Y. Tomioka, Y. Matusi, and Y. Tokura, *Phys. Rev. Lett.* **90**, 177203 (2003).
- ⁴³N. Vandewalle, M. Ausloos, and R. Cloots, *Phys. Rev. B* **59**, 11909 (1999).
- ⁴⁴H. L. Ju and H. Sohn, *Solid State Commun.* **102**, 463 (1997).
- ⁴⁵P. Dey and T. K. Nath, *Phys. Rev. B* **73**, 214425 (2006).
- ⁴⁶P. K. Siwach, U. K. Goutam, P. Srivastava, H. K. Singh, R. S. Tiwari, and O. N. Srivastava, *J. Phys. D* **39**, 14 (2006).
- ⁴⁷J. Mucha, *J. Phys.: Condens. Matter* **18**, 1427 (2006).
- ⁴⁸F. J. Blatt, *Physics of Electronic Conduction Ion Solids* (McGraw-Hill, New York, 1968).
- ⁴⁹S. N. Barilo, G. L. Bychkov, L. A. Kurnevich, S. V. Shiryayev, L. A. Kurochkin, J. W. Lynn, and L. Vasiliu-Doloc, *J. Cryst. Growth* **211**, 480 (2000).
- ⁵⁰N. F. Mott and E. A. Davies, *Electronic Processes in Noncrystalline Solids*, 2nd ed. (Oxford University Press, New York, 1979).
- ⁵¹D. N. Tsygankov and A. L. Efros, arXiv:cond-mat/0106094.
- ⁵²S. Pal, A. Banerjee, E. Rozenberg, and B. K. Chaudhuri, *J. Appl. Phys.* **89**, 4955 (2001).
- ⁵³Y. Yuzhelevski, V. Markovich, V. Dikovskiy, E. Rozenberg, G. Gorodetsky, G. Jung, D. A. Shulyatev, and Ya. M. Mukovskii, *Phys. Rev. B* **64**, 224428 (2001).
- ⁵⁴P. Raychaudhuri, P. Taneja, S. Sarkar, A. K. Nigam, P. Ayyub, and R. Pinto, arXiv:cond-mat/9805231v1.
- ⁵⁵N. Mott, *Conduction in Non-Crystalline Materials* (Clarendon, Oxford, 1993).
- ⁵⁶B. F. Woodfield, M. L. Wilson, and J. M. Beyers, *Phys. Rev. Lett.* **78**, 3201 (1997).
- ⁵⁷M. Viret, L. Ranno, and J. M. D. Coey, *Phys. Rev. B* **55**, 8067 (1997).
- ⁵⁸M. Jaime, H. T. Hardner, M. B. Salamon, M. Rubinstein, P. Dorsey, and D. Emin, *Phys. Rev. Lett.* **78**, 951 (1997).
- ⁵⁹M. Jaime, M. B. Salamon, M. Rubinstein, R. E. Treece, J. S. Horwitz, and D. B. Chrissey, *Phys. Rev. B* **54**, 11914 (1996).
- ⁶⁰M. Jaime, P. Lin, S. H. Chun, M. B. Salamon, P. Dorsey, and M. Rubinstein, *Phys. Rev. B* **60**, 1028 (1999).
- ⁶¹N. D. Mathur, G. Burnell, S. P. Isaac, T. J. Jackson, B. S. Teo, J. L. MacManus-Driscoll, L. F. Cohen, J. E. Evetts, and M. G. Blamire, *Nature (London)* **387**, 266 (1997).